HHS Public Access

Author manuscript

Biochemistry. Author manuscript; available in PMC 2020 May 13.

Published in final edited form as:

Biochemistry. 2018 July 03; 57(26): 3976–3986. doi:10.1021/acs.biochem.8b00511.

Reassessment of the Transport Mechanism of the Human Zinc Transporter SLC39A2

Marie C. Franz[#†,‖], **Jonai Pujol-Giménez**[#†], **Nicolas Montalbetti**[†,⊥], **Miguel Fernandez-Tenorio**[‡], **Timothy R. DeGrado**[§], **Ernst Niggli**[‡], **Michael F. Romero**[§], **Matthias A. Hediger**[*,†]

[†] University of Bern, Institute of Biochemistry and Molecular Medicine, and National Center of Competence in Research, NCCR TransCure, Bühlstrasse 28, 3012 Bern, Switzerland [‡] University of Bern, Department of Physiology, Buehlplatz 5, 3012 Bern, Switzerland [§] Department of Physiology and Biomedical Engineering, Mayo Clinic College of Medicine and Science, Rochester, Minnesota 55905, United States

[#] These authors contributed equally to this work.

Abstract

The human zinc transporter SLC39A2, also known as ZIP2, was shown to mediate zinc transport that could be inhibited at pH <7.0 and stimulated by HCO_3^-, suggesting a Zn^{2+}/HCO_3^- cotransport mechanism [Gaither, L. A., and Eide, D. J. (2000) *J. Biol. Chem. 275*, 5560–5564]. In contrast, recent experiments in our laboratory indicated that the functional activity of ZIP2 increases at acidic pH [Franz, M. C., et al. (2014) *J. Biomol. Screening 19*, 909–916]. The study presented here was therefore designed to reexamine the findings about the pH dependence and to extend the functional characterization of ZIP2. Our current results show that ZIP2-mediated transport is modulated by extracellular pH but independent of the H^+ driving force. Also, in our experiments, ZIP2-mediated transport is not modulated by extracellular HCO_3^-. Moreover, a high extracellular [K^+], which induces depolarization, inhibited ZIP2-mediated transport, indicating that the transport mechanism is voltage-dependent. We also show that ZIP2 mediates the uptake of Cd^{2+} (K_m ~ 1.57 μM) in a pH-dependent manner (K_{H^+} ~ 66 nM). Cd^{2+} transport is inhibited by extracellular [Zn^{2+}] (IC_{50} ~ 0.32 μM), [Cu^{2+}] (IC_{50} ~ 1.81 μM), and to a lesser extent [Co^{2+}], but not by [Mn^{2+}] or [Ba^{2+}]. Fe^{2+} is not transported by ZIP2. Accordingly, the substrate selectivity of ZIP2 decreases in the following order: $Zn^{2+} > Cd^{2+} \geq Cu^{2+} > Co^{2+}$. Altogether, we propose that ZIP2 is a facilitated divalent metal ion transporter that can be modulated by extracellular pH and membrane potential. Given that ZIP2 expression has been reported in acidic environments [Desouki, M. M., et al. (2007) *Mol. Cancer 6*, 37; Inoue, Y., et al. (2014) *J. Biol. Chem. 289*, 21451–21462; Tao, Y. T., et al. (2013) *Mol. Biol. Rep. 40*, 4979–4984], we suggest that the herein described H^+-mediated regulatory mechanism might be important for determining the velocity and direction of the transport process.

[*]**Corresponding Author:** Institute of Biochemistry and Molecular Medicine, University of Bern, Bühlstrasse 28, 3012 Bern, Switzerland. Telephone: +41 31 631 41 29. Matthias.hediger@ibmm.unibe.ch.

[‖]M.C.F.: CSL Behring, Wankdorfstrasse 10, 3014 Bern, Switzerland.

[⊥]N.M.: Department of Medicine, University of Pittsburgh, 3550 Terrace St., Pittsburgh, PA 15261.

The authors declare no competing financial interest.

Graphical Abstract

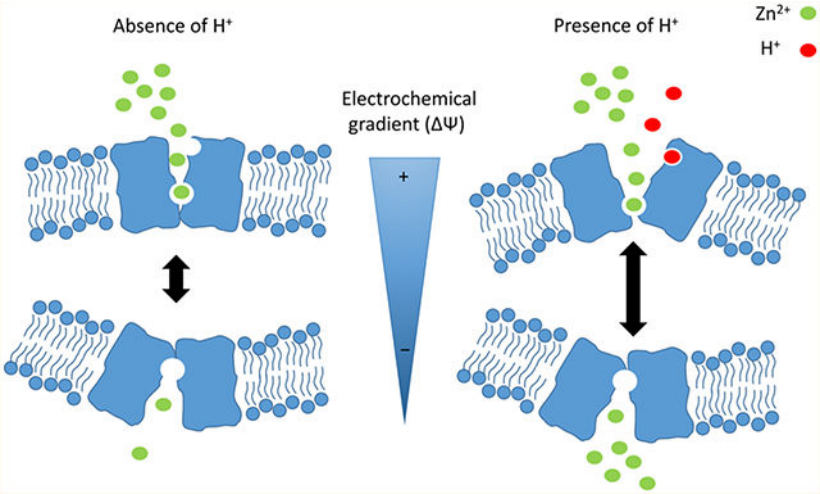

Zinc is an essential trace element for human nutrition and the second most abundant transition element after iron in living organisms. The importance of zinc becomes evident when looking at a recent bioinformatics analysis indicating that as much as 10% of the human proteome is potentially capable of binding zinc.[6] More than 3000 different types of proteins require zinc as a key structural or catalytic component. Among them are transcription factors, signaling proteins, transport/storage proteins, zinc finger proteins, and proteins involved in DNA repair, replication, and translation.[7] Whole body and cellular zinc homeostasis is being thoroughly regulated. Whereas systemic zinc intoxication is relatively rare, zinc deficiency is a widespread problem leading to growth retardation, cognitive impairment, and immune dysfunction.[8] The maintenance of mammalian zinc homeostasis is achieved by high-affinity zinc transport systems that are regulated by metal sensors.[7] There are at least two different solute carrier (SLC) families of zinc transporters that control the movement of Zn^{2+} across membranes: (1) the SLC30 zinc transporter family, also known as the ZnT family, that facilitates cellular efflux or uptake into intracellular compartments and (2) the SLC39 family, also known as the ZIP family, that facilitates cellular uptake or efflux from intracellular compartments.[9–12]

The mammalian SLC39/ZIP family consists of 14 members, which can be divided into four subfamilies based on sequence similarity. SLC39A2 (ZIP2) together with SLC39A1 (ZIP1) and SLC39A3 (ZIP3) comprises subfamily II. ZIP2 was originally cloned and characterized by Gaither and Eide in 2000.[1] In this study, they showed that more $^{65}Zn^{2+}$ accumulated in ZIP2-expressing K562 cells than in parental cells, in a time-, temperature-, and concentration-dependent manner. They found that ZIP2-mediated zinc transport was not dependent on ATP hydrolysis or on Na^+ or K^+ gradients. In their assay, ZIP2 was inhibited at acidic pH (<7.0) and stimulated by 0.5 mM HCO_3^-. Thus, they proposed a Zn^{2+}/HCO_3^- cotransport mechanism. In the same study, the expression level of *ZIP2* mRNA was found to be generally low or negligible in human tissues and cultured cell lines, except in prostate and uterus,[1] where it indeed could also be detected at the protein level.[3] Cao et al. found *ZIP2* mRNA in peripheral blood mononuclear cells (PBMCs) and monocytes.[13] In their study,

zinc depletion in both cell lines triggered upregulation of *ZIP2* with concomitant downregulation of zinc-binding metallothioneins. Recently, Inoue et al. detected ZIP2 in the epidermis of healthy human frozen skin samples.[4] They discovered that ZIP2 was upregulated by differentiation induction of cultured keratinocytes. Interestingly, ZIP2 knockdown inhibited the differentiation of keratinocytes and consequently the formation of a three-dimensional cultured epidermis. Several studies have linked the downregulation of ZIP2 in prostatic tissue to decreased zinc levels in prostatic epithelial cells and to prostate cancer.[3,14–18] Studies with ZIP2-KO mice did not reveal any specific phenotype. However, these mice were more susceptible to abnormal embryonic development because of zinc deficiency during pregnancy.[19]

Recently, we published a screening assay that was established using the FLIPR Tetra high-throughput microplate reader to identify specific modulators of ZIP2 as potential therapeutic hit or lead compounds.[2] This assay is based on the use of a Ca^{2+}-sensitive dye, Calcium 5 (Molecular Devices), which, in addition to Ca^{2+}, binds Cd^{2+} with high affinity. Binding of either Ca^{2+} or Cd^{2+} to the dye induces emission of a fluorescent signal that can be monitored, allowing quantification of the transport activity of proteins that mediate Cd^{2+} influx, such as ZIP2, which transports Cd^{2+} efficiently.[1,2] In our laboratory, this assay has been successfully used to monitor the activity of a variety of Cd^{2+}-transporting proteins such as the human divalent metal transporter DMT1 (SLC11A2)[20] or the epithelial calcium channel TRPV6.[21] Interestingly, during the development of the assay, we discovered discrepancies between our results on ZIP2 transport characteristics and the originally reported functional characterization of ZIP2.[1] Therefore, the goal of the current work was to reexamine and extend the functional characterization of ZIP2.

MATERIALS AND METHODS

Chemicals and Reagents

Unless mentioned, all the chemicals and reagents were purchased from Sigma-Aldrich.

Cell Culture Methods

HEK293 cells were grown in complete Dulbecco’s modified Eagle’s medium (Gibco) supplemented with 10% fetal bovine serum (FBS), 10 mM HEPES, 100 μM minimal essential medium non-essential amino acids, and 1 mM sodium pyruvate (Gibco). Cells were cultured at 37 °C and 5% CO_2 and subcultivated when confluency reached 90%.

Cells were transfected 24 h after being plated, following the manufacturer’s protocol for the Lipofectamine 2000 (Invitrogen) reagent, using 50% of the recommended amount of human SLC39A2/ZIP2 (UniProt entry Q9NP94) encoding DNA and Lipofectamine 2000. The transfection medium was changed after 4 h. The transfection efficiency was estimated to be at least 70% using fluorescence microscopy.

Cd^{2+}-Flux Measurements Using the FLIPR Tetra

Cells were plated in 96-well, clear-bottom, black-well plates coated with poly-D-lysine at a density of 2×10^4 cells/well. The next day, cells were transfected with ZIP2-pIRES2 DsRed-

Express2 or mock-transfected using lipotransfection. On the experimental day, the cell culture medium was replaced with 100 μL of loading buffer [modified Krebs buffer containing 117 mM NaCl, 4.8 mM KCl, 1 mM $MgCl_2$, 10 mM D-glucose, 5 mM HEPES, 5 mM MES, and Calcium 5 fluorescence dye (Molecular Devices) (pH 6.5)]. Cells were then incubated in the loading buffer at 37 °C for 1 h. Fluorescence measurements were taken using a FLIPR-Tetra high-throughput fluorescence microplate reader. Cells were excited using the 470–495 nm LED module, and the emitted fluorescence signal was filtered with a 515–575 nm emission filter. Cd^{2+} and the other tested solutes were prepared in assay buffer as 2× concentrated solutions in a separate 96-well plate. Establishment of a stable baseline was followed by addition of 100 μL of the indicated [Cd^{2+}] and measurements of fluorescence for 15 min. Measurements were taken at 1 s intervals. In the negative control group, no substrate was administered. Results were exported from the FLIPR raw data as the "area under the curve" (AUC) of the fluorescence signal intensity in the interval after the addition of substrates (460–750 s). In sodium replacement experiments, 120 msssM NaCl was replaced with 120 mM choline chloride, NMDG, or KCl. In chloride replacement assays, all the chloride-containing salts were replaced by their corresponding equimolar gluconate salts. In pH dependence experiments, the different pH values were adjusted with 1 N HCl/NaOH.

Oocyte Isolation and Injection

Capped cRNA was synthesized using a linearized cDNA template and the T7 mMessage mMachine kit (Ambion). *Xenopus laevis* oocytes were isolated and dissociated using collagenase as described previously[22] followed by injection with 50 nL of water or cRNA at 0.4 ng/nL (20 ng/oocyte), using a Nanoject-II injector (Drummond Scientific, Broomall, PA). Oocytes were maintained at 16 °C in OR3 medium[22] and studied 3–6 days after injection.

Radioactive Uptake

The uptake of zinc by oocytes was measured by incubating groups of 8–10 *X. laevis* oocytes for 30 min in 1 mL of uptake buffer [ND96: 96 mM NaCl, 2 mM KCl, 1 mM $MgCl_2$, 1.8 mM $CaCl_2$, 5 mM MES, 1 mM HEPES, and 1 mM Tris (pH 6.0)] with 100 μM $ZnCl_2$ including 0.05 μCi of $^{63}Zn^{2+}$ (prepared as reported in ref 23). Oocytes were washed three times in uptake buffer with 1 mM $ZnCl_2$ before measurement of incorporation of $^{63}Zn^{2+}$ into single oocytes as γ emission with a WIZARD2 gamma counter (PerkinElmer). For $^{63}Zn^{2+}$ uptake at different pH values, the amounts of MES, HEPES, and Tris were varied. To determine the effect of HCO_3^- on ZIP2 function, 96 mM NaCl was replaced with 96 mM $NaHCO_3$ in the standard ND96. In sodium replacement assays, 96 mM NaCl was replaced with 96 mM choline chloride or 96 mM KCl.

Radioactive iron uptake experiments in HEK293 cells were performed as described previously.[20] Briefly, cells were plated in 96-well, clear-bottom, white-well plates coated with poly-Dlysine at a density of 2×10^4 cells/well. The next day, cells were transfected with ZIP2-pIRES2 DsRed-Express2 or hDMT1-pIRES2 DsRed-Express2 using lipotransfection. On the experimental day, the growth medium was aspirated and cells were washed three times with Krebs−Ringer buffer [140 mM NaCl, 2.5 mM KCl, 1.2 mM $MgCl_2$,

1.2 mM $CaCl_2$, 10 mM D-glucose, 5 mM HEPES, and 5 mM MES (pH 7.4)]. To measure iron uptake, Krebs−Ringer buffer (pH 5.5) was supplemented with 1 mM ascorbic acid, 1 μM $FeCl_2$, and 5 μCi/mL radioactive ^{55}Fe (American Radiolabeled Chemicals). The assay was terminated after 15 min when the plates were washed four times with ice-cold Krebs −Ringer buffer. Subsequently, 100 μL of MicroScint-20 (PerkinElmer) was dispensed into each well and incubated at RT for 1 h under constant agitation. Radioactive ^{55}Fe uptake was measured using a TopCount Microplate Scintillation and Luminescence Counter (PerkinElmer).

Two-Electrode Voltage Clamp

Two-microelectrode voltage clamping (TEVC) was used to measure steady-state currents in control oocytes and oocytes injected with ZIP2 mRNA, 4–7 days after injection. Oocyte membrane currents were recorded using an OC-725C voltage clamp (Warner Instruments, Hamden, CT), filtered at 2–5 kHz, digitized at 10 kHz, and recorded with Pulse software, and data were analyzed using the PulseFit program (HEKA), as previously described.[22] Voltage microelectrodes (resistance of 0.5–5 MΩ) were made from fiber-capillary borosilicate and filled with 3 M KCl. Oocytes were perfused at room temperature in ND96 buffer. For periods when current−voltage (*I-V*) protocols were not being run, oocytes were clamped at a holding potential (V_h) of −60 mV. *I-V* protocols consisted of 100 ms step changes in membrane potential from −120 to 40 mV in 20 mV increments before and after the addition of the test substrate. The resulting data were filtered at 5 kHz (eight-pole Bessel filter, Frequency Devices) and sampled at 1 kHz. The *I-V* relationship was determined by plotting the mean steady-state current against the voltage for a given set of experiments. Additionally, the current was monitored continuously in oocytes clamped at a V_h of −60 mV. Test solutions were perfused at room temperature for several minutes until a steady-state current was observed.

pH Microelectrodes

Ion-selective microelectrodes were used to monitor the intracellular pH (pH_i) of ZIP2- and water-injected oocytes as previously described.[22] Ion-selective electrodes were pulled like those used for TEVC and silanized with bis(dimethylamino)-dimethylsilane (Fluka Chemical Corp., Ronkonkoma, NY). Electrode tips were filled with hydrogen ionophore 1-cocktail B (Fluka) and backfilled with phosphate buffer at pH 7.0. The intracellular pH was measured as the difference between the pH electrode and a KCl voltage electrode impaled into the oocyte, and the membrane potential (V_m) was the potential difference between the KCl and an extracellular calomel microelectrode. Electrodes were calibrated using pH 6.0 and 8.0 (Fisher), followed by point calibration in ND96 (pH 7.50). All pH microelectrodes used had slopes of at least −54 mV/pH unit.

Confocal Cd^{2+}-Flux Imaging: A Single Cell with Clamped Membrane Potential (patch clamping)

The membrane potential was clamped to −60 mV using the patchclamp technique in the whole-cell configuration. The pipet solution was composed of 120 mM Cs-Asp, 20 mM TEA-Cl, 5 mM K_2ATP, 8 mM NaCl, 5.6 mM $MgCl_2$ (0.75 mM free Mg^{2+}), 20 mM HEPES, and 50 μM Fluo 3 pentapotassium salt. Note that, for this experimental set, to monitor Cd^{2+}

fluxes, the Calcium 5 dye was replaced with Fluo 3, another calcium indicator that is sensitive to Cd^{2+},[24] because a membrane impermeable dye was required to avoid unspecific signal loss after cell loading. The pH was adjusted to 7.2 with CsOH, and the osmolality was 285 mosmol/kg. The external solution was composed of 117 mM NaCl, 4.8 mM KCl, 1 mM $MgCl_2$, 5 mM D-glucose, 5 mM HEPES, and 5 mM MES. The pH was adjusted to 6.5 with 1 N HCl. Under high-potassium conditions, NaCl was replaced with equimolar KCl. All experiments were performed at room temperature.

Confocal Cd^{2+} Imaging: Multicell Recording

Calcium 5 fluorescent dye (Molecular Devices) was used to record Cd^{2+} uptake. Prior to the measurements, cells were incubated for 1 h at 37 °C in the following external solution: 117 mM NaCl, 4.8 mM KCl, 1 mM $MgCl_2$, 10 mM D-glucose, 5 mM HEPES, 5 mM MES, and Calcium 5 dye. The pH was adjusted to 6.5 with 1 N HCl. Under high-potassium conditions, NaCl was replaced with equimolar KCl. All experiments were performed at room temperature.

Cd^{2+} images were acquired with a FluoView 1000 (Olympus) confocal laser-scanning microscope. Fluo 3 and Calcium 5 dye were excited at 473 nm with a solid-state laser, and fluorescence was detected between 515 and 585 nm. To control cell transfection, DsRed-Express2 was excited at 561 or 488 nm with a solid-state laser and fluorescence was detected at >585 nm. Images were processed and analyzed using the software ImageJ. The measurements are expressed as $\Delta F/F_0$, where F_0 is the fluorescence recorded before the application of Cd^{2+}.

Statistical Analyses

The normal distribution of the experimental groups was determined by Kolmogorov −Smirnov ($N > 50$) and Shapiro−Wilk ($N < 50$) tests. Normally distributed independent experimental groups were compared with an unpaired Student's t test. When the data sets were not normally distributed, a Mann−Whitney U test was used to assess differences. Statistical tests were performed using the IBM statistics 20 software. P values of <0.05 are considered statistically significant.

RESULTS

Dependence of ZIP2 Functional Activity on Extracellular pH

On the basis of the studies of Gaither et al., the functional activity of ZIP2 was found to be inhibited at pH <7.0.[1] On the other hand, our fluorescence-based transport assay using transiently transfected HEK293 cells revealed that, at acidic pH (6.5), the level of ZIP2-mediated Cd^{2+} transport was greatly increased compared to that at pH 7.5.[2] What could be the reason for this discrepancy? In our assay, pH changes may have influenced the binding affinity of the fluorescent dye used (Calcium 5) to measure Cd^{2+}. Also, Cd^{2+} rather than Zn^{2+} transport was measured, which might account for the reversed pH dependence. We therefore decided to perform additional experiments to evaluate this incongruity. To this end, we used the standard radioactive tracer method using *X. laevis* oocytes as an expression system, thus ensuring the same functional readout that was used by Gaither et al. Using this

methodology, the effect of variable extracellular pH values (pH 5.0–8.2) on ZIP2-mediated $^{63}Zn^{2+}$ uptake was determined (Figure 1A). Whereas the water-injected oocytes showed only a slight pH dependence of endogenous Zn^{2+} transport activity, ZIP2 transport activity was maximal at an acidic pH of <6.0 and almost negligible at pH >7.5. These results confirmed our previous findings[2] and further validate our fluorescence assay that was used as a screening assay to identify ZIP2 modulators.

Zn^{2+} Transport Mediated by ZIP2 Is Not Coupled to HCO_3^-

It was previously proposed that ZIP2 operates as a Zn^{2+}/HCO_3^- cotransporter.[1] We aimed to confirm this hypothesis by measuring the uptake of $^{63}Zn^{2+}$ by ZIP2 cRNA-microinjected *X. laevis* oocytes in the presence and absence of HCO_3^-. To this end, we replaced the [NaCl] of the uptake solution by an equimolar [$NaHCO_3$], which resulted in a pH of 8.2. Because adjusting the pH of the solution would alter [HCO_3^-], we compared the $^{63}Zn^{2+}$ uptake in the HCO_3^--containing solution with that in the normal uptake solution, both at pH 8.2 (Figure 1B). We did not observe a difference in the transport activity of ZIP2, whereas the H_2O-injected oocytes showed a higher activity at increased HCO_3^- concentrations. Additionally, to confirm these findings, we used pH-sensitive microelectrodes to measure intracellular pH (pH_i) changes due to HCO_3^--coupled Zn^{2+} transport via ZIP2expressed *X. laevis* oocytes (Figure 2A). The uptake buffer was equilibrated by addition of 5% CO_2 and 33 mM HCO_3^-. The CO_2 caused an acidification in ZIP2-injected oocytes (Figure 2A,C) as well as in H_2O-injected oocytes (data not shown). Upon perfusion of Zn^{2+}, the pH_i did not change, contrary to what would be expected if the transport was coupled to HCO_3^- (Figure 2A,C).

ZIP2 Does Not Transport H^+

Our experiments suggest that H^+ may be involved in the ZIP2-mediated transport process. Thus, we also used the pH-sensitive microelectrodes in *X. laevis* oocytes to investigate whether protons are coupled to ZIP2-mediated Zn^{2+} transport (Figure 2B). Almost no change was observed when the pH 7.5 uptake solution was replaced by the pH 6 solution, indicating that there is no H^+ permeation via ZIP2. Also, addition of Zn^{2+} did not cause a significant change in pH_i in ZIP2-injected oocytes (Figure 2B,C). These results indicate that ZIP2 does not facilitate transport of H^+, neither alone nor coupled to Zn^{2+} transport.

ZIP2 Is Not Electrogenic

To test whether ZIP2-mediated Zn^{2+} transport is electrogenic, functional experiments were performed using two-electrode voltage clamping (TEVC). We did not observe any discernible change in the current−voltage (*I-V*) relationship following step changes in membrane potential (V_m) of oocytes expressing ZIP2 at extracellular pH 7.5 or 6.0 (Figure 3A,B). Moreover, perfusion of Zn^{2+} (100 μM) did not evoke any appreciable change in the *I-V* relationship (Figure 3A,B). Similar results were obtained when the current was monitored continuously in oocytes clamped (V_h) at −60 mV (data not shown). Hence, functional experiments performed with TEVC indicate that there are no measurable currents associated with ZIP2-mediated Zn^{2+} transport, which is surprising, given the positive charge of the divalent metal ion Zn^{2+} and the highly significant transport activity observed for ZIP2 cRNA-injected oocytes when measuring $^{63}Zn^{2+}$ accumulation under similar experimental conditions (Figure 1).

Transport Mediated by ZIP2 Is Not Dependent on Na^+ or Cl^- Gradients but Is Inhibited by K^+

We investigated whether ZIP2-mediated transport is coupled to Na^+, K^+, or Cl^- by isosmotic replacement of these ions in the standard uptake solution. To address this question, we used both a fluorescentbased Cd^{2+} influx assay (Figure 4A) in transiently transfected HEK293 cells and a $^{63}Zn^{2+}$ uptake assay in ZIP2 cRNA-injected *X. laevis* oocytes (Figure 4B). Na^+ was replaced by equimolar NMDG, choline, or K^+, whereas Cl^- was replaced by the corresponding gluconate salts. Replacement of Na^+ with NMDG or choline had no effect on ZIP2 activity, whereas replacing it by K^+ reduced the rate of transport by ≈60–40%. Replacement of chloride by gluconate salts did not have any effect on ZIP2 activity.

Transport Mediated by ZIP2 Is Not Coupled to K^+ but Is Voltage-Dependent

To clarify whether the decrease in the rate of ZIP2-mediated Cd^{2+} or Zn^{2+} transport when Na^+ is replaced with K^+ is due to direct K^+-coupled metal ion transport or merely a result of membrane depolarization generated by an increased extracellular [K^+], fluorometric analysis under voltage-clamp conditions was conducted. First, fluorometric measurements were taken without voltage clamping, within an open field of ZIP2-transfected cells (Figure 5A–C). In line with our previous observations, replacement of Na^+ with equimolar K^+ induced ≈40% inhibition of the ZIP2-mediated influx of Cd^{2+}. Next, the same procedure was performed in individual cells under voltage-clamp conditions (V_h = −60 mV) (Figure 5D–F). Interestingly, under voltage-clamp conditions, the inhibition was lost and the ZIP2-mediated influx of Cd^{2+} was similar in the presence and absence of a high extracellular [K^+]. These results demonstrate that K^+ is not part of the translocation mechanism of ZIP2 and that transport is voltage-dependent.

Transport Kinetics and pH Dependence of ZIP2

The kinetics of ZIP2-mediated transport was studied using our Cd^{2+}-flux fluorescence-based assay in transiently transfected HEK293 cells. Fluorescence intensity changes increased with extracellular [Cd^{2+}] (Figure 6A, top panel). Measuring Cd^{2+} flux through ZIP2 gave a dose −response curve that reached saturation at 5 μM Cd^{2+} (Figure 6C). The calculated apparent affinity constant (K_m) for Cd^{2+} was ~1.57 ± 018 μM. Empty vector-transfected cells did not show any change in fluorescence intensity within the tested range of Cd^{2+} concentrations (Figure 6A, bottom panel).

Using the same methodology, the pH dependence of the ZIP2-mediated transport was studied. In line with our previous findings, fluorescence intensity changes after Cd^{2+} (10 μM) perfusion increased with extracellular [H^+] (Figure 6B, top panel). Transport was completely saturated at extracellular pH 6.5, and the calculated apparent affinity (K_{H^+}) was ~66 ± 16 nM, corresponding to pH ~7.2 (Figure 6C). Again, no effect was observed over the empty vector-transfected cells (Figure 6B, bottom panel).

Cation Selectivity of ZIP2

To investigate the cationic selectivity of ZIP2, Cd^{2+} flux was measured in the presence of high extracellular concentrations (50 μM) of different divalent cations such as Ba^{2+}, Mn^{2+}, Co^{2+}, Zn^{2+}, and Cu^{2+} (Figure 7A). Note that none of these metal ions showed significant

interactions with the Calcium 5 dye when high concentrations of them (100 μM) were perfused individually into ZIP2-overexpressing cells (data not shown). As expected, in the presence of Zn^{2+}, Cd^{2+} flux was completely inhibited. Interestingly, Cu^{2+} and Co^{2+} inhibited 75 and 25%, respectively, of the Cd^{2+} flux, while no significant inhibition by Ba^{2+} or Mn^{2+} was observed. Fe^{2+} is another putative substrate of ZIP2. However, because it also interacts with the Calcium 5 dye, it was not included in this set of experiments. To overcome this issue, we measured directly radiolabeled iron ($^{55}Fe^{2+}$) uptake (Figure 7B). As a positive control for this assay, we used human divalent metal transporter 1 (hDMT1, SLC11A2).[25] Uptake of $^{55}Fe^{2+}$ by ZIP2 was not significantly different from that of empty vector-transfected cells and 7-fold lower than the uptake mediated by hDMT1, demonstrating that Fe^{2+} is not a substrate of ZIP2.

To determine the apparent affinity of ZIP2 for Zn^{2+} and Cu^{2+}, Cd^{2+} flux was measured in the presence of a range of extracellular concentrations of Zn^{2+} or Cu^{2+}. In both cases, inhibition of Cd^{2+} flux gave dose−response sigmoidal curves. The calculated IC_{50} values were ~0.52 ± 1.7 μM for Zn^{2+} (Figure 7C) and ~2.98 ± 1.3 μM for Cu^{2+} (Figure 7D). Given that the K_m of ZIP2 for Cd^{2+} is 1.57 μM (Figure 6C), according to the Cheng−Prusoff equation,[26] the IC_{50} values for Zn^{2+} and Cu^{2+} are 0.32 and 1.81 μM, respectively. Hence, the cationic selectivity for ZIP2 decreases in the following order: $Zn^{2+} > Cd^{2+} \geq Cu^{2+} > Co^{2+}$. Fe^{2+}, Mn^{2+}, and Ba^{2+} are not transport substrates.

DISCUSSION

In our functional experiments using different approaches, the level of ZIP2-mediated transport was increased at acidic pH, even though no cotransport with H^+ was observed. We therefore conclude that the ZIP2 transport process is modulated by extracellular pH, independent of the H^+ driving force. Transport was not stimulated by the presence of HCO_3^-, as previously reported.[1] Thus, we conclude that ZIP2-mediated transport is not coupled to bicarbonate. Also, in contrast to the previous observations,[1] our experiments revealed that an increasing extracellular [K^+] inhibits ZIP2-mediated metal ion uptake under non-voltage-clamp conditions. However, when the K^+ inhibitory effect was measured under voltage-clamp conditions, it was abolished. This indicates that the inhibitory effect was due do the depolarization caused by increasing the extracellular K^+ concentration to 140 mM. Therefore, we concluded that ZIP2-mediated metal ion transport is voltagedependent, and given the positive charge of Zn^{2+}, we expected that transport would be electrogenic.

Paradoxically, our electrophysiological analysis revealed that ZIP2-mediated Zn^{2+} transport is electroneutral. The electrophysiological experiments were performed with ZIP2 overexpressed in *X. laevis* oocytes and in the presence of a robust inwardly directed electrochemical Zn^{2+} gradient, favoring transmembrane influx (i.e., the membrane voltage was kept constant at −60 mV and 100 μM $ZnCl_2$ was perfused). Using the same experimental approach, our group observed prominent transmembrane inward currents for Fe^{2+} transport via DMT1 expressed in *X. laevis* oocytes, even at neutral pH (that is in the absence of an inwardly directed H^+ gradient).[27] Given that ZIP2-injected oocytes exhibited a high level of ^{63}Zn accumulation as shown in Figure 1, this rules out any issue related to plasma membrane expression. To explain the lack of electrogenicity, we propose the

following: (1) Transport is still electrogenic, but the turnover rate of the transport process is too slow to allow any detection of transport-associated currents. (2) Transport is electroneutral because there is an as yet unidentified coupling ion (via cotransport or exchange) that balances the positive charges of Zn^{2+}. In this case, given the voltage dependence of the transport process, the transport cycle must contain steps that are limited by the membrane potential.

Interestingly, the transport features of ZIP2 resemble those of a ZIP transporter from the Gram-negative, rod-shaped bacterium *Bordetella bronchiseptica* (ZIPB).[28] In that work, ZIPB was described as a selective electrodiffusional channel, in which Zn^{2+} uptake is driven only down its concentration gradient. Remarkably, Zn^{2+} transport by ZIPB was modulated by the effect of K^+ on the resting membrane potential, indicating that ZIPB is also voltage-dependent. Furthermore, ZIPB-mediated Zn^{2+} flux was modulated by pH and not stimulated by HCO_3^-. Also in line with our findings, *Fugu* pufferfish ZIP2, sharing 30 and 60% sequence identity with human ZIP2 and ZIP3, respectively, exhibited, when expressed in MDCK cells, Zn^{2+}-mediated transport in a pH-dependent manner. Transport was stimulated by acidic pH medium (pH 5.5–6.5) but was not enhanced (but rather slightly inhibited) by the presence of extracellular HCO_3^-.[29]

Altogether, given that ZIP2-mediated transport is ATP-independent[1] and not coupled to Na^+, H^+, K^+, HCO_3^-, or Cl^-, we propose that Zn^{2+} uptake occurs via simple passive transport. Given that Zn^{2+} is a trace element essential for most mammalian cells, efficient uptake mechanisms must exist to allow Zn^{2+} to accumulate within cells. Because intracellular Zn^{2+} is complexed with specific binding proteins, cytoplasmic Zn^{2+} concentrations are kept at very low (femtomolar to picomolar) levels. Consequently, the inwardly directed electrochemical Zn^{2+} gradient is expected to be sufficient to facilitate cellular Zn^{2+} uptake, supporting this concept of passive ZIP2-mediated transport.[28]

The only ion showing interaction with the transport process mediated by ZIP2 is H^+. Our results show that, at low extracellular pH values, the rate of transport of Zn^{2+} is increased. However, H^+ was not cotransported with Zn^{2+}, and there was transport at pH >7.5, indicating that ZIP2-mediated transport is modulated by pH, rather than H^+ acting as a coupling ion. In addition to the aforementioned ZIPB and *Fugu* pufferfish ZIP2, there are many examples of ion channels that can be modulated by external pH, including Cl^- channels,[30] Na^+ channels,[31] and aquaporins,[32] among others.[33] In these channels, the protonation state of specific titratable residues affects voltage dependence or gate opening, leading to modulation of channel permeation. Future structure−function studies of ZIP2 to identify amino acid residues responsible for H^+ sensitivity will shed further light on this pH modulatory mechanism.

As described previously, ZIP2 expression has been found in prostate epithelial cells,[34] peripheral blood mononuclear cells of patients with tuberculosis and asthma,[5] and epidermal keratinocytes.[4] Interestingly, these tissues and/or cell types are involved in physiological processes occurring in an acidic environment. The main function of the prostate is to secrete prostatic fluid, which is acidic (pH 6.5–6.7).[34,35] On the basis of its apical membrane localization, ZIP2 is hypothesized to help maintain prostate Zn^{2+} homeostasis by

reabsorbing Zn^{2+} from the prostatic fluid.[3] Similarly, acidification of the airways linked to different pathological processes, including inflammation, ischemia or aspiration of refluxing gastric contents, and obstructive airway diseases such as asthma, may lead to an increased rate of ZIP2-mediated transport.[33] ZIP2 expression has been described in the epidermis, and moreover, transportermediated Zn^{2+} uptake is necessary for the differentiation of keratinocytes.[4] The surface of healthy skin has a pH oscillating between 4.0 and 6.0.[36] Altogether, these findings further support the role of H^+ in the transport processes mediated by ZIP2 because, as our functional experiments point out, the functional activity of ZIP2 will be increased in these acidic environments. In turn, it seems counterintuitive to use HCO_3^- as a driving force for the transport of Zn^{2+} under such physiological conditions as, at reduced pH, a significant part of bicarbonate will be in the conjugated acid form carbonic acid (H_2CO_3) (pK_a = 6.1 at 37 °C). In this regard, upregulation of ZIP2 expression in peripheral blood mononuclear cells of patients with tuberculosis was accompanied by downregulation of the expression of SLC39A8 (ZIP8), and the authors proposed that this could be a consequence of changes in the pH and Zn^{2+} concentrations.[5] These findings suggest a complementary function of ZIP2 and ZIP8. In line with this, our preliminary experiments using the fluorescence-based assay described herein revealed opposite pH modulation for ZIP8 and ZIP2 (data not shown).

With respect to the kinetic properties of ZIP2, our experiments indicate that the K_m for ZIP2-mediated Cd^{2+} flux was ~1.6 μM, similar to that reported by Gaither and Eide for Zn^{2+} (K_m ~ 3 μM).[1] On the other hand, on the basis of our assay, ZIP2-mediated transport reached V_{max} already at 5 μM Cd^{2+}, whereas in the study by Gaither et al., the V_{max} for Zn^{2+} transport was 20–40 μM.[1] Another difference between the two studies exists upon comparison of the divalent metal competition experiments. According to our experiments, ZIP2 can transport Zn^{2+} and Cd^{2+} but not Fe^{2+} and Cu^{2+} and Co^{2+} are likely also substrates, while Ba^{2+} and Mn^{2+} were not transported by ZIP2. In contrast, Gaither et al. proposed that all of these metals ions could serve as substrates of ZIP2.[1] In line with our findings, studies with HEK293 cells overexpressing mouse ZIP2 showed similar Michaelis−Menten kinetics for Zn^{2+} (K_m ~ 1.6 μM).[37] Moreover, Zn^{2+} transport was inhibited in this study by excesses of Cu^{2+}, Cd^{2+}, and Co^{2+} but not Fe^{2+} or Mn^{2+}. In contrast, the previously mentioned pufferfish ZIP2 exhibited a 10-fold lower affinity for Zn^{2+} (K_m ~ 13 μM), while Zn^{2+} transport was inhibited by Cu^{2+}, Cd^{2+}, Co^{2+}, Fe^{3+}, and to a lesser extent Fe^{2+}.[29] This variability among competition experiments highlights the importance of determining the substrate selectivity of transporters by direct measurements of each putative substrate. In this regard, direct measurements of ^{63}Zn (Figures 1 and 4B), Cd^{2+}(Figure 6), and Fe uptake (Figure 7B) confirm that Zn^{2+} and Cd^{2+} are real substrates of ZIP2, while iron was not found to be a substrate. With regard to the other proposed ZIP2 substrates (i.e., Cu^{2+} and Co^{2+}), direct measurements will also be required to verify they are transport substrates.

The incongruities between this work and that of Gaither et al. are likely due to the use of different expression systems. Gaither et al. used the chronic myeloid leukemia cell line K562 for their radiolabeled Zn^{2+} uptake experiments. These cells endogenously express Zn^{2+} transporters, as well as the sodium− proton exchanger NHE1 (SLC9A1)[38] and the chloride/ bicarbonate anion exchanger AE2 (SLC4A2).[39] Thus, the reported Zn^{2+} transport activities and divalent metal ion specificities in K652 cells represent the sum of both endogenous and

expressed ZIP2 transporters. In addition, the inverse pH sensitivity and role of bicarbonate in ZIP2-mediated transport could be related to interfering activities of NHE1 and AE2. Our functional experiments were conducted in HEK293 cells, which express endogenous NHE3 (SLC9A1)[40] but not AE2.[41] Also, experiments were performed in *Xenopus* oocytes, which express an NHE exchanger homologue but not any endogenous anionic exchangers.[42] As functional readouts, we used a combination of different methods, including electrophysiological measurements, radiolabeled Zn^{2+} uptake experiments in *X. laevis* oocytes, and a Cd^{2+}-flux-based fluorescent assay in HEK293 cells. Importantly, in non-injected control oocytes or in empty vector-transfected HEK cells, endogenous Zn^{2+} transport (Figure 1) or Cd^{2+} transport (Figure 6A) was negligible compared to that of ZIP2-expressing oocytes or cells. Hence, our experimental approaches guarantee an optimal signal-to-noise ratio for studying different aspects of the ZIP2 transport mechanism. This allowed us to validate our observations using different techniques, thereby generating data with great consistency, as demonstrated, for example, for the pH dependence (Figures 1A and 6B) or the effect of K^+ (Figures 4 and 5).

We anticipate that the data reported herein are valuable for predicting the putative roles of ZIP2 in pathological situations or during physiological challenges. Indeed, human genetic studies revealed that ZIP2 polymorphisms constitute a risk factor for a wide variety of human diseases, including carotid artery disease in aging,[43] arsenic-related bladder cancer,[44] and cystic fibrosis.[45] In addition, ZIP2 activity is important for prostate function and related to prostate cancer development,[3,34] keratinocyte differentiation,[4] and macrophage[46] and monocyte function.[13] Also, ZIP2 knockout mice studies revealed increased susceptibility to Zn deficiency during pregnancy.[19] As a follow-up, specific experiments are needed to identify the particular roles of ZIP2 in physiologically relevant environments. For example, functional studies with the aforementioned genetic variants will be required to reveal the precise molecular mechanisms leading to the associated disease conditions. Also, tissue specific knockout studies in cellular or animal models are required to describe the physiological and pathological impacts of ZIP2 dysfunction. Such studies may in turn accelerate the discovery of therapeutic applications targeting ZIP2.

CONCLUSION

Our data show that ZIP2-mediated transport is modulated by extracellular pH, in an H^+ driving force-independent and voltage-dependent manner. Accordingly, we propose that ZIP2 is a facilitative transporter that mediates transport of Zn^{2+} down its concentration gradient, which can be modulated by interaction of H^+ with titratable acidic amino acid residues within the ZIP2 protein. Specifically, we propose that protonation of such a titratable amino acid stabilizes the ZIP2 protein in a conformation in which substrate transport is more favorable. This would explain why the transport rate is increased in the presence of H^+. ZIP2 is expressed in acidic environments, where this regulatory mechanism is expected to be important to accelerate and determine the direction of the transport process.

The herein proposed transport mechanism is consistent with those of ZIPs from lower organisms (i.e., ZIPB and pufferfish ZIP2).[28,29] Nevertheless, this does not necessarily hold true for all the ZIP members, as some of them have been postulated to possess different

transport mechanisms. For example, ZIP8 and ZIP14 are described as metal/bicarbonate symporters.[47,48] In this regard, as mentioned previously, a preliminary experiment from our laboratory, monitoring Cd^{2+} fluxes through human ZIP8-overexpressing cells, showed that the activity of this transporter is not stimulated by extracellular H^+, indicating a transport mechanism that is different from that for ZIP2 described herein. This highlights the need for future studies for each ZIP family member individually, to reveal their particular transport mechanisms and to understand their distinctive contributions to body Zn^{2+} homeostasis.

ACKNOWLEDGMENTS

The authors highlight and thank Tamara Locher and Yvonne Amrein (laboratory of M. A. Hediger) for their dedication and technical support.

Funding

J.P.-G. was funded by the Marie Curie Actions International Fellowship Program (IFP) TransCure (www.nccr-transcure.ch). Supported by the Swiss National Science Foundation (SNSF) grant # 31003A_156376 to M.A.H, the SNSF National Center of Competence in Research grant NCCR TransCure # 51NF40_125762, the SNSF grant # 310030–156375 to E.N. and the Microscopy Imaging Facility of the University of Bern (MIC). We also thank Drs. Mukesh K. Pandey and Aditya Bansal from the Radiology group of the Mayo Clinic (laboratory of T. R. DeGrado) for their help during the performance of the $^{63}Zn^{2+}$ Isotope flux studies.

ABBREVIATIONS

ZIP	ZrT/Irt-like protein
HEK293	human embryonic kidney 293
HEPES	4-(2-hydroxyethyl)-1-piperazineethanesulfonic acid
MES	2-(*N*-morpholino) ethanesulfonic acid
NMDG	*N*-methyl-D-glucamine
Tris	2-amino-2-(hydroxymethyl)propane-1,3-diol
RT	room temperature
Cs-Asp	cesium aspartate
TEA-Cl	tetraethylammonium chloride
K_2ATP	adenosine 5′-triphosphate dipotassium salt
cRNA	complementary RNA
pH_i	intracellular pH
TEVC	two-electrode voltage clamping
I-V	current−voltage
V_m	membrane potential
V_h	holding voltage

ZIPB	B. *bronchiseptica* ZrT/Irt-like protein
MDCK	Madin-Darby canine kidney
SD	standard deviation

REFERENCES

(1). Gaither LA, and Eide DJ (2000) Functional expression of the human hZIP2 zinc transporter. J. Biol. Chem 275, 5560–5564. [PubMed: 10681536]

(2). Franz MC, Simonin A, Graeter S, Hediger MA, and Kovacs G (2014) Development of the First Fluorescence Screening Assay for the SLC39A2 Zinc Transporter. J. Biomol. Screening 19, 909–916.

(3). Desouki MM, Geradts J, Milon B, Franklin RB, and Costello LC (2007) hZip2 and hZip3 zinc transporters are down regulated in human prostate adenocarcinomatous glands. Mol. Cancer 6, 37. [PubMed: 17550612]

(4). Inoue Y, Hasegawa S, Ban S, Yamada T, Date Y, Mizutani H, Nakata S, Tanaka M, and Hirashima N (2014) ZIP2 protein, a zinc transporter, is associated with keratinocyte differentiation. J. Biol. Chem 289, 21451–21462. [PubMed: 24936057]

(5). Tao YT, Huang Q, Jiang YL, Wang XL, Sun P, Tian Y, Wu HL, Zhang M, Meng SB, Wang YS, Sun Q, and Zhang LY (2013) Up-regulation of Slc39A2(Zip2) mRNA in peripheral blood mononuclear cells from patients with pulmonary tuberculosis. Mol. Biol. Rep 40, 4979–4984. [PubMed: 23686108]

(6). Andreini C, Banci L, Bertini I, and Rosato A (2006) Counting the zinc-proteins encoded in the human genome. J. Proteome Res 5, 196–201. [PubMed: 16396512]

(7). Maret W, and Li Y (2009) Coordination dynamics of zinc in proteins. Chem. Rev 109, 4682–4707. [PubMed: 19728700]

(8). Brown KH, Peerson JM, Rivera J, and Allen LH (2002) Effect of supplemental zinc on the growth and serum zinc concentrations of prepubertal children: a meta-analysis of randomized controlled trials. Am. J. Clin. Nutr 75, 1062–1071. [PubMed: 12036814]

(9). Eide DJ (2006) Zinc transporters and the cellular trafficking of zinc. Biochim. Biophys. Acta, Mol. Cell Res 1763, 711–722.

(10). Palmiter RD, and Huang L (2004) Efflux and compartmentalization of zinc by members of the SLC30 family of solute carriers. Pfluegers Arch. 447, 744–751. [PubMed: 12748859]

(11). Jeong J, and Eide DJ (2013) The SLC39 family of zinc transporters. Mol. Aspects Med 34, 612–619. [PubMed: 23506894]

(12). Liuzzi JP, and Cousins RJ (2004) Mammalian zinc transporters. Annu. Rev. Nutr 24, 151–172. [PubMed: 15189117]

(13). Cao J, Bobo JA, Liuzzi JP, and Cousins RJ (2001) Effects of intracellular zinc depletion on metallothionein and ZIP2 transporter expression and apoptosis. J. Leukocyte Biol 70, 559–566. [PubMed: 11590192]

(14). Rishi I, Baidouri H, Abbasi JA, Bullard-Dillard R, Kajdacsy-Balla A, Pestaner JP, Skacel M, Tubbs R, and Bagasra O (2003) Prostate cancer in African American men is associated with downregulation of zinc transporters. Appl. Immunohistochem Mol. Morphol 11, 253–260. [PubMed: 12966353]

(15). Franz MC, Anderle P, Bürzle M, Suzuki Y, Freeman MR, Hediger MA, and Kovacs G (2013) Zinc transporters in prostate cancer. Mol. Aspects Med 34, 735–741. [PubMed: 23506906]

(16). Costello LC, Franklin RB, Zou J, Feng P, Bok R, Swanson MG, and Kurhanewicz J (2011) Human prostate cancer ZIP1/zinc/citrate genetic/metabolic relationship in the TRAMP prostate cancer animal model. Cancer Biol. Ther 12, 1078–1084. [PubMed: 22156800]

(17). Franklin RB, Feng P, Milon B, Desouki MM, Singh KK, Kajdacsy-Balla A, Bagasra O, and Costello LC (2005) hZIP1 zinc uptake transporter down regulation and zinc depletion in prostate cancer. Mol. Cancer 4, 32. [PubMed: 16153295]

(18). Johnson LA, Kanak MA, Kajdacsy-Balla A, Pestaner JP, and Bagasra O (2010) Differential zinc accumulation and expression of human zinc transporter 1 (hZIP1) in prostate glands. Methods 52, 316–321. [PubMed: 20705137]

(19). Hara T, Takeda TA, Takagishi T, Fukue K, Kambe T, and Fukada T (2017) Physiological roles of zinc transporters: molecular and genetic importance in zinc homeostasis. J. Physiol. Sci 67, 283–301. [PubMed: 28130681]

(20). Montalbetti N, Simonin A, Dalghi MG, Kovacs G, and Hediger MA (2014) Development and Validation of a Fast and Homogeneous Cell-Based Fluorescence Screening Assay for Divalent Metal Transporter 1 (DMT1/SLC11A2) Using the FLIPR Tetra. J. Biomol. Screening 19, 900–908.

(21). Kovacs G, Montalbetti N, Simonin A, Danko T, Balazs B, Zsembery A, and Hediger MA (2012) Inhibition of the human epithelial calcium channel TRPV6 by 2-aminoethoxydiphenyl borate (2-APB). Cell Calcium 52, 468–480. [PubMed: 23040501]

(22). Romero MF, Fong P, Berger UV, Hediger MA, and Boron WF (1998) Cloning and functional expression of rNBC, an electrogenic Na(+)-HCO3- cotransporter from rat kidney. Am. J. Physiol 274, F425–432. [PubMed: 9486238]

(23). DeGrado TR, Pandey MK, Byrne JF, Engelbrecht HP, Jiang H, Packard AB, Thomas KA, Jacobson MS, Curran GL, and Lowe VJ (2014) Preparation and preliminary evaluation of 63Zn-zinc citrate as a novel PET imaging biomarker for zinc. J. Nucl. Med 55, 1348–1354. [PubMed: 25047329]

(24). Oyama Y, Arata T, Chikahisa L, Soeda F, and Takahama K (2002) Estimation of increased concentration of intracellular Cd(2+) by fluo-3 in rat thymocytes exposed to CdCl(2). Environ. Toxicol. Pharmacol 11, 111–118. [PubMed: 21782592]

(25). Pujol-Gimenez J, Hediger MA, and Gyimesi G (2017) A novel proton transfer mechanism in the SLC11 family of divalent metal ion transporters. Sci. Rep 7, 6194. [PubMed: 28754960]

(26). Yung-Chi C, and Prusoff WH (1973) Relationship between the inhibition constant (K1) and the concentration of inhibitor which causes 50% inhibition (I50) of an enzymatic reaction. Biochem. Pharmacol 22, 3099–3108. [PubMed: 4202581]

(27). Mackenzie B, Ujwal ML, Chang MH, Romero MF, and Hediger MA (2006) Divalent metal-ion transporter DMT1 mediates both H+ -coupled Fe2+ transport and uncoupled fluxes. Pfluegers Arch. 451, 544–558. [PubMed: 16091957]

(28). Lin W, Chai J, Love J, and Fu D (2010) Selective electrodiffusion of zinc ions in a Zrt-, Irt-like protein, ZIPB. J. Biol. Chem 285, 39013–39020. [PubMed: 20876577]

(29). Qiu A, and Hogstrand C (2005) Functional expression of a low-affinity zinc uptake transporter (FrZIP2) from pufferfish (Takifugu rubripes) in MDCK cells. Biochem. J 390, 777–786. [PubMed: 15907194]

(30). Chen MF, and Chen TY (2001) Different fast-gate regulation by external Cl(−) and H(+) of the muscle-type ClC chloride channels. J. Gen. Physiol 118, 23–32. [PubMed: 11429442]

(31). Kang IS, Cho JH, Choi IS, Kim DY, and Jang IS (2016) Acidic pH modulation of Na+ channels in trigeminal mesencephalic nucleus neurons. NeuroReport 27, 1274–1280. [PubMed: 27755281]

(32). Chauvigne F, Zapater C, Stavang JA, Taranger GL, Cerda J, and Finn RN (2015) The pH sensitivity of Aqp0 channels in tetraploid and diploid teleosts. FASEB J. 29, 2172–2184. [PubMed: 25667219]

(33). Holzer P (2009) Acid-sensitive ion channels and receptors. Handb. Exp. Pharmacol 194, 283–332.

(34). Franz MC, Anderle P, Burzle M, Suzuki Y, Freeman MR, Hediger MA, and Kovacs G (2013) Zinc transporters in prostate cancer. Mol. Aspects Med 34, 735–741. [PubMed: 23506906]

(35). Charalabopoulos K, Karachalios G, Baltogiannis D, Charalabopoulos A, Giannakopoulos X, and Sofikitis N (2003) Penetration of antimicrobial agents into the prostate. Chemotherapy 49, 269–279. [PubMed: 14671426]

(36). Boer M, Duchnik E, Maleszka R, and Marchlewicz M (2016) Structural and biophysical characteristics of human skin in maintaining proper epidermal barrier function. Postępy dermatologii i alergologii 33, 1–5.

(37). Dufner-Beattie J, Langmade SJ, Wang F, Eide D, and Andrews GK (2003) Structure, function, and regulation of a subfamily of mouse zinc transporter genes. J. Biol. Chem. 278, 50142–50150. [PubMed: 14525987]

(38). Lane DJ, Robinson SR, Czerwinska H, and Lawen A (2010) A role for Na+/H+ exchangers and intracellular pH in regulating vitamin C-driven electron transport across the plasma membrane. Biochem. J 428, 191–200. [PubMed: 20307259]

(39). Vigliarolo T, Zocchi E, Fresia C, Booz V, and Guida L (2016) Abscisic acid influx into human nucleated cells occurs through the anion exchanger AE2. Int. J. Biochem. Cell Biol 75, 99–103. [PubMed: 27015766]

(40). Lang K, Wagner C, Haddad G, Burnekova O, and Geibel J (2003) Intracellular pH activates membrane-bound Na(+)/H(+) exchanger and vacuolar H(+)-ATPase in human embryonic kidney (HEK) cells. Cell. Physiol. Biochem 13, 257–262. [PubMed: 14586169]

(41). Yabuuchi H, Tamai I, Sai Y, and Tsuji A (1998) Possible role of anion exchanger AE2 as the intestinal monocarboxylic acid/ anion antiporter. Pharm. Res 15, 411–416. [PubMed: 9563070]

(42). Sobczak K, Bangel-Ruland N, Leier G, and Weber WM (2010) Endogenous transport systems in the Xenopus laevis oocyte plasma membrane. Methods 51, 183–189. [PubMed: 19963061]

(43). Giacconi R, Muti E, Malavolta M, Cardelli M, Pierpaoli S, Cipriano C, Costarelli L, Tesei S, Saba V, and Mocchegiani E (2008) A novel Zip2 Gln/Arg/Leu codon 2 polymorphism is associated with carotid artery disease in aging. Rejuvenation Res. 11, 297–300. [PubMed: 18328005]

(44). Karagas MR, Andrew AS, Nelson HH, Li Z, Punshon T, Schned A, Marsit CJ, Morris JS, Moore JH, Tyler AL, Gilbert-Diamond D, Guerinot ML, and Kelsey KT (2012) SLC39A2 and FSIP1 polymorphisms as potential modifiers of arsenic-related bladder cancer. Hum. Genet 131, 453–461. [PubMed: 21947419]

(45). Kamei S, Fujikawa H, Nohara H, Ueno-Shuto K, Maruta K, Nakashima R, Kawakami T, Matsumoto C, Sakaguchi Y, Ono T, Suico MA, Boucher RC, Gruenert DC, Takeo T, Nakagata N, Li JD, Kai H, and Shuto T (2018) Zinc Deficiency via a Splice Switch in Zinc Importer ZIP2/SLC39A2 Causes Cystic FibrosisAssociated MUC5AC Hypersecretion in Airway Epithelial Cells. EBioMedicine 27, 304–316. [PubMed: 29289532]

(46). Hamon R, Homan CC, Tran HB, Mukaro VR, Lester SE, Roscioli E, Bosco MD, Murgia CM, Ackland ML, Jersmann HP, Lang C, Zalewski PD, and Hodge SJ (2014) Zinc and zinc transporters in macrophages and their roles in efferocytosis in COPD. PLoS One 9, e110056. [PubMed: 25350745]

(47). Girijashanker K, He L, Soleimani M, Reed JM, Li H, Liu Z, Wang B, Dalton TP, and Nebert DW (2008) Slc39a14 gene encodes ZIP14, a metal/bicarbonate symporter: similarities to the ZIP8 transporter. Mol. Pharmacol 73, 1413–1423. [PubMed: 18270315]

(48). He L, Girijashanker K, Dalton TP, Reed J, Li H, Soleimani M, and Nebert DW (2006) ZIP8, member of the solutecarrier-39 (SLC39) metal-transporter family: characterization of transporter properties. Mol. Pharmacol 70, 171–180. [PubMed: 16638970]

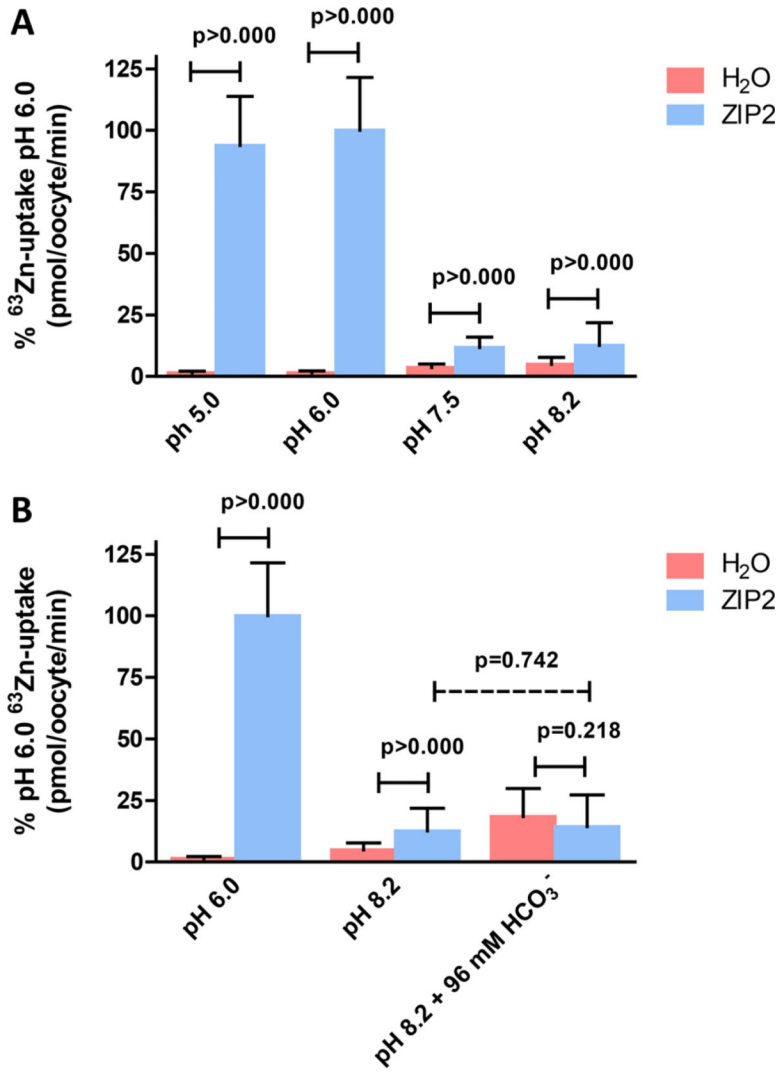

Figure 1.

Effect of extracellular pH and bicarbonate upon $^{63}Zn^{2+}$ uptake by ZIP2-expressing *X. laevis* oocytes. Uptake of $^{63}Zn^{2+}$ in the presence of 100 μM $ZnCl_2$ by ZIP2- and H_2O-injected *X. laevis* oocytes was measured (A) at different extracellular pH values (5–8.2) and (B) in the absence (pH 6 and 8.2) and presence of HCO_3^- (96 mM) at pH 8.2. Data from three different batches of oocytes were normalized to the mean Zn^{2+} uptake by ZIP2 at pH 6.0 (580 ± 124 to 403 ± 62 pmol oocyte^{-1} min^{-1}) and are represented as means ± SD (6–26 oocytes).

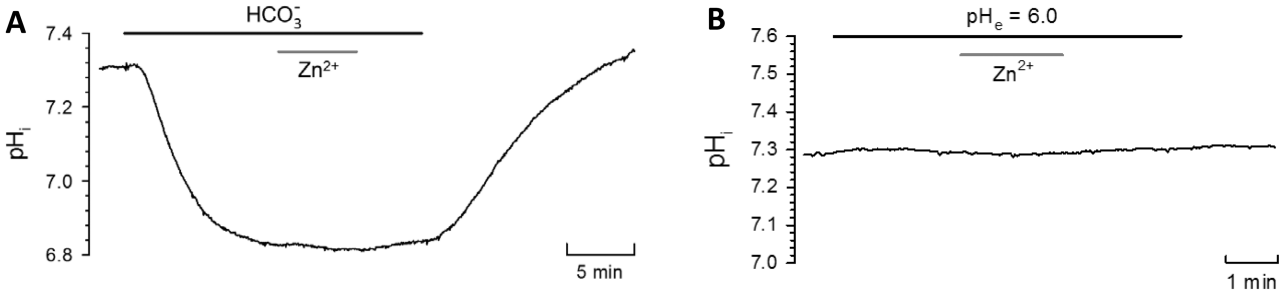

C

	ND96 pH 7.5	ND96 pH 7.5 5% CO2 / 33mM HCO_3^-	ND96 pH 7.5 5% CO2 / 33mM HCO_3^- + Zn^{2+}	ND96 pH 6.0	ND96 pH 6.0 + Zn^{2+}
Initial pH_i	7.275 ± 0.17	-	-	-	-
pH change $d(pH_i)$	-	-0.395 ± 0.119	-0.006 ± 0.022	0.017 ± 0.018	-0.005 ± 0.004
pH slope $\Delta(pH_i)/dt$ (x 10^{-5} pH_i/s)	-	-160.3 ± 58	-6.9 ± 17.3	32.1 ± 21.1	-1.2 ± 2.8

Figure 2.

Role of bicarbonate and protons in zinc uptake by ZIP2-expressing *X. laevis* oocytes. Representative trace of intracellular pH (pH_i) changes in response to perfusion of (A) CO_2 (5%) and HCO_3^- (33 mM) or (B) ND96 at pH 6.0 in the absence and presence of Zn^{2+} (100 μM). Transport activity of ZIP2 was monitored as the change in pH_i when Zn^{2+} was added and removed extracellularly. (C) Summary of the pH change and pH slope (10^{-5} pH unit/s) determined after the perfusion of each of the different media. Results are means ± SD (2–6 oocytes).

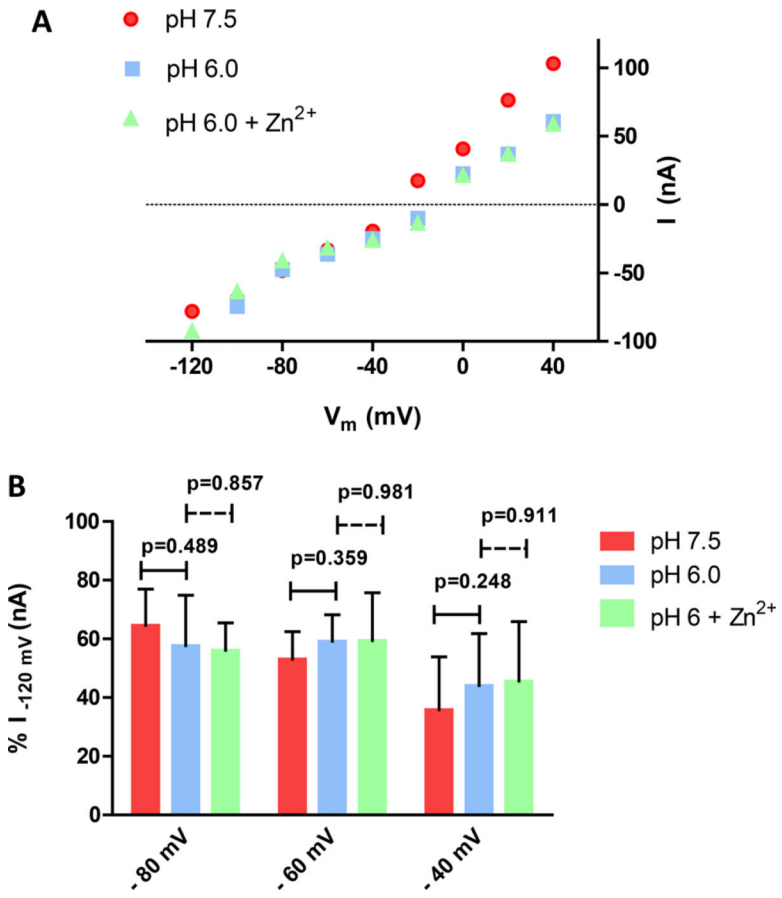

Figure 3.

Electrophysiological properties of ZIP2-expressing *X. laevis* oocytes. (A) Representative trace of the current−voltage relationship under the indicated conditions (V_h = −60 mV; 100 μM Zn^{2+}). (B) Average currents recorded under the indicated conditions. For each individual oocyte, the data were normalized to the current recorded at −120 mV in pH 7.5 medium (−159.37 to −38.75 nA). Data from the different oocytes (n = 6) were pooled together and are represented as means ± SD.

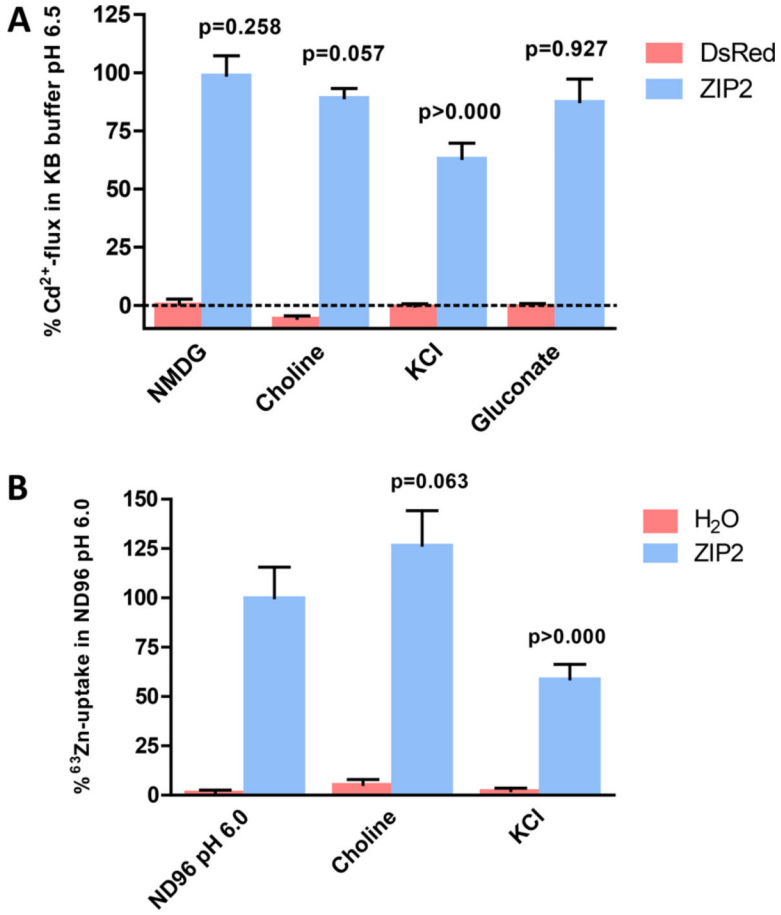

Figure 4.

Effect of sodium, chloride, and potassium extracellular concentration on ZIP2 transport activity. (A) Changes in fluorescence intensity of Calcium 5 dye in response to Cd^{2+} perfusion (1 μM) measured in HEK293 cells transiently transfected with DsRed-Express2 and ZIP2 DNA constructs in KB buffer (pH 6.5) in which extracellular Na^+ or Cl^- was replaced with equimolar NMDG, choline$^+$, and K^+ or gluconate salts, respectively. Data from two independent experiments were normalized to the mean ZIP2 activity at pH 6.5 and are represented as means ± SD (n = 8–12). (B) Uptake of $^{63}Zn^{2+}$ in the presence of 100 μM $ZnCl_2$ by ZIP2- and H_2O-injected *X. laevis* oocytes measured in ND96 (pH 6.0) in which extracellular Na^+ was replaced with equimolar choline$^+$ or K^+. Data from two different batches of oocytes were normalized to the mean Zn^{2+} uptake by ZIP2 at pH 6.0 (403 ± 62 pmol oocyte^{-1} min^{-1}) and are represented as means ± SD (6–12 oocytes). *P* values establish statistical differences between hZIP2-mediated Zn^{2+} uptake at pH 6.0 and the indicated experimental conditions.

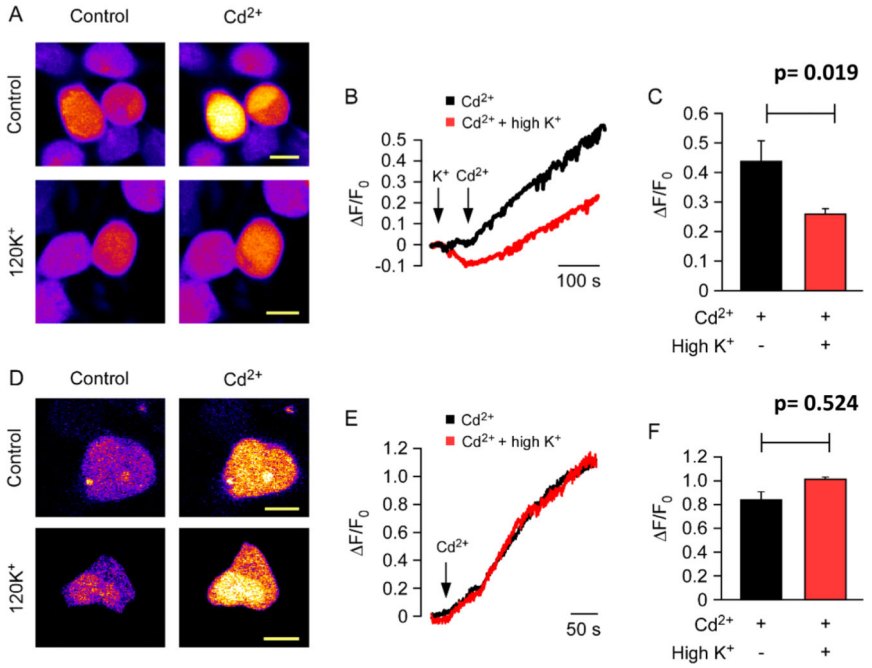

Figure 5.

Effect of potassium on membrane potential in ZIP2 transiently transfected HEK293 cells. Representative images of (A) intact or (D) dialyzed cells before and after the treatment with Cd^{2+} (10 μM) in the presence (control) or absence of extracellular 120 mM K^+. Representative traces of Cd^{2+}-flux-induced changes in fluorescence intensity in (B) intact and (E) clamped cells in the presence and absence of 120 mM K^+. Fluorescence intensity changes were measured as $\Delta F/F_0$ (where F_0 is the signal before application of Cd^{2+}). Data from three and five independent experiments for intact (n = 38–41) and dialyzed (n = 8–10) cells, respectively, are represented as means ± SD.

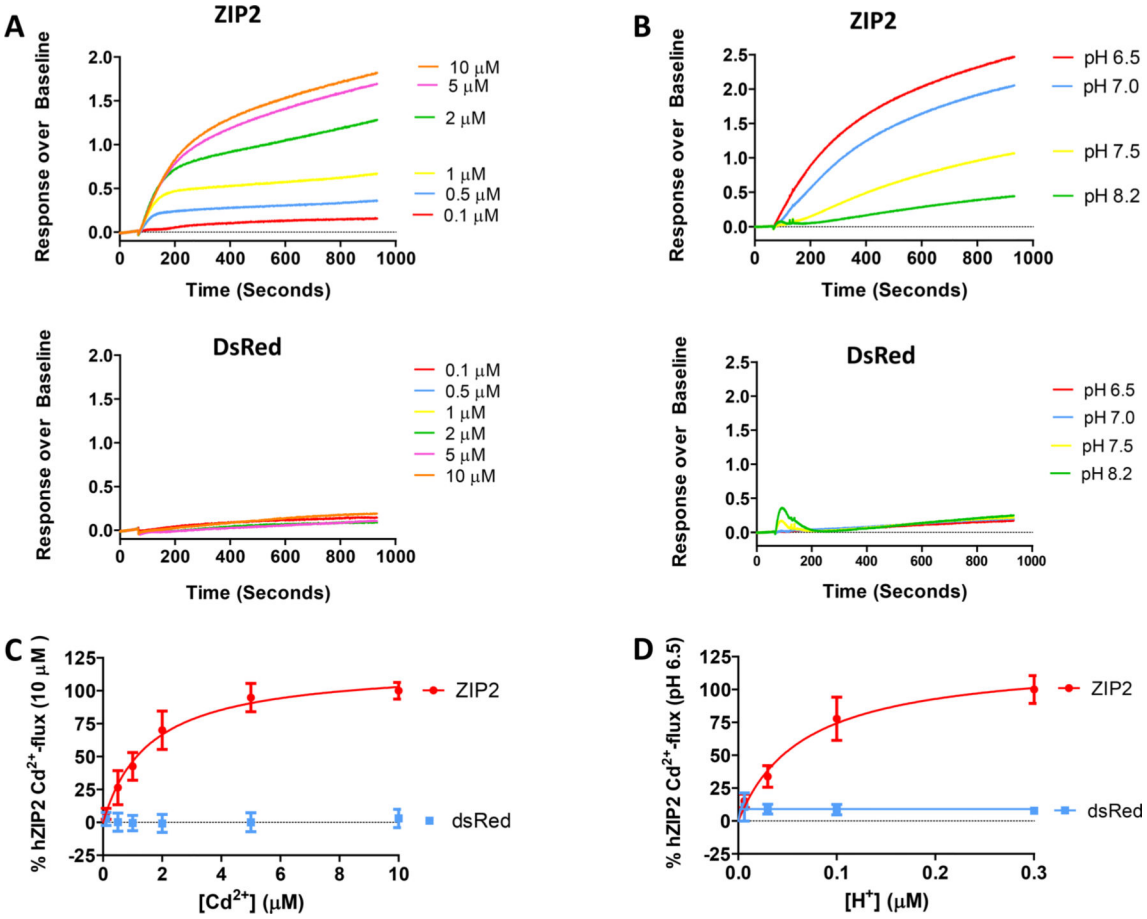

Figure 6.

Kinetics and pH dependence of the Cd^{2+} transport measured in ZIP2 or DsRed-Express2 (empty vector) transiently transfected HEK293 cells. Representative experiments showing the changes in fluorescence intensity of Calcium 5 dye in response to the perfusion of different Cd^{2+} concentrations (0.1–10 μM) at extracellular pH 6.5 (A) or at different extracellular pH values (6.5–8.2) in the presence of a saturating concentration of Cd^{2+} (10 μM) (B). To determine the kinetics (C) and pH dependence (D) of Cd^{2+} transport, the AUC for each single trace was calculated. Data from three independent experiments were normalized to the mean Cd^{2+} uptake by ZIP2 at pH 6.5 (337.22 ± 34 to 890 ± 22 AUC) and collected and are represented as means ± SD (n = 7–28). Kinetic parameters were obtained by fitting the data points to the Michaelis−Menten equation (solid lines).

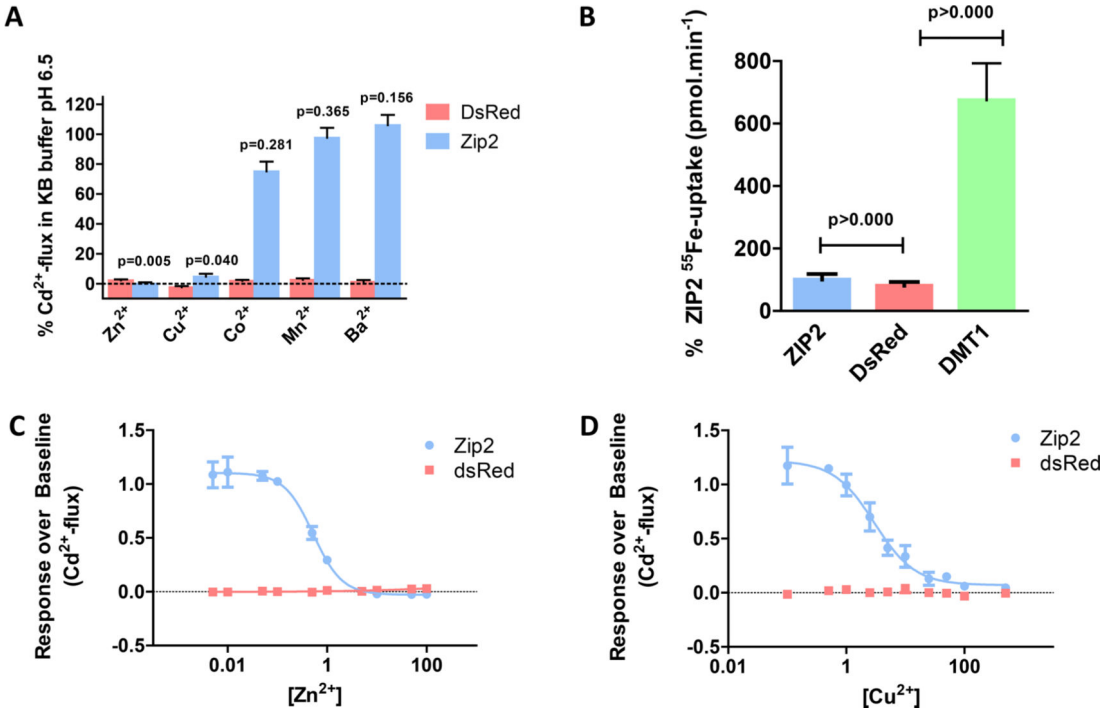

Figure 7.

Divalent cation selectivity of ZIP2 in transiently transfected HEK293 cells. (A) Changes in fluorescence intensity of Calcium 5 dye in response to Cd^{2+} perfusion (1 μM) measured in the presence of the indicated divalent cations (50 μM) at pH 6.5. Data from two independent experiments were normalized to the mean ZIP2 activity at pH 6.5 in the absence of divalent cations other than Cd^{2+} (1 μM) and are represented as means ± SD (n = 5–8). P values establish statistical differences between ZIP2-mediated Cd^{2+} uptake in the absence and presence of the indicated divalent metals. (B) Uptake of $^{55}Fe^{2+}$ in the presence of 1 μM $FeCl_2$ and 100 μM ascorbic acid by HEK293 cells transiently transfected with ZIP2, DsRed-Express2 (empty vector) and DMT1 DNA constructs at extracellular pH 5.5. Data from two independent experiments were normalized to the mean ZIP2 $^{55}Fe^{2+}$ transport (0.09 ± 0.01 to 0.15 ± 0.02 pmol min^{-1}) and are represented as means ± SD (n = 19−48). Inhibition of the ZIP2-mediated Cd^{2+} transport (1 μM) by increasing extracellular [Zn^{2+}] (C) and [Cu^{2+}] (D). Data from two independent experiments were normalized to the mean ZIP2 activity at pH 6.5 in the absence of divalent cations other than Cd^{2+} and are represented as means ± SD (n = 7). Inhibitory kinetics were obtained by fitting the data points to a four-parameter sigmoidal equation (solid lines).